Chiral permselectivity in nanoporous opal films surface-modified with chiral selector moieties

ARTICLE *in* JOURNAL OF MATERIALS CHEMISTRY · MAY 2007

Impact Factor: 7.44 · DOI: 10.1039/B617607K

2 AUTHORS, INCLUDING:

Ilya Zharov
University of Utah
77 PUBLICATIONS **1,484** CITATIONS

Chiral permselectivity in nanoporous opal films surface-modified with chiral selector moieties†

Julie Cichelli and Ilya Zharov*

Received 4th December 2006, Accepted 5th March 2007
First published as an Advance Article on the web 21st March 2007
DOI: 10.1039/b617607k

The chiral permselectivity in thin opal films modified on the silica surface with chiral selector moieties was studied as a function of opal film geometry, supporting electrolyte concentration, solvent polarity, and chiral selector and linker structure. While opal film thickness, supporting electrolyte concentration and linker length and structure did not have a significant influence on the chiral permselectivity, the nanopore size, solvent polarity and selector structure had a pronounced effect. These observations are in agreement with the chiral selectivity mechanism in the opal films in which the permeating enantiomers are transported with different rates through the surface utilizing non-covalent interactions between the chiral permeant molecules and surface-bound chiral selectors. The chiral selectivity (transport rate ratio for *S* and *R* enantiomers) achieved in the present study was 4.5, which is one of the highest reported for chiral membranes.

Introduction

The past decade has seen increasing interest in the preparation of enantiomerically pure compounds. This interest was intensified by an FDA statement concerning the development of chiral drugs as single enantiomers.[1] Separation of racemic mixtures (*e.g.*, by crystallization) is presently the most widely used method of producing single enantiomers in industry. A variety of other chiral separation techniques exists including chromatography and electrophoresis, but they only allow a small amount of material to be separated per run, their scale-up is expensive and such methods are not energy- and cost-efficient. Membrane separations, on the other hand, constitute a promising method that can be operated under ambient conditions.[2–4]

The common feature of chiral membrane separations is that they are based on the difference in non-covalent binding energy between each enantiomer and a selector molecule,[5–7] or on the preferential inclusion into a cavity within a polymer or a porous material.[8] Presently used enantioselective membranes[9–12] usually consist of a non-selective porous material either supporting a liquid phase containing chiral selector molecules,[11] or carrying selector moieties on its surface. In the latter type of enantioselective membranes, which are much more robust compared to the liquid membranes, selector moieties can be introduced by coating the pores with a thin layer of a chiral polymer,[13] by covalently grafting the selector to the membrane,[14–18] by preparing a porous polymeric film that incorporates chiral selectors,[19–21] or by molecularly imprinting a polymer.[10,18,22] Recently, optically active polyelectrolyte multilayer membranes have been shown to separate enantiomers.[23] It has also been shown that nanotube membranes surface-modified with antibodies allow enantioselective separations.[24,25]

To be practical, chiral membranes require a high surface area, low mass transfer resistance, good mechanical strength and selectivity. Nanoporous opal membranes may provide an ideal medium for chiral separations. Indeed, synthetic opals form *via* self-assembly of silica nanospheres into a close-packed face-centered cubic (fcc) lattice with a void fraction of 0.26 independent of the size of the spheres.[26] The opals contain highly ordered arrays of three-dimensional interconnected nanopores whose size can be controlled by changing the size of the silica spheres used to assemble the opal, and whose surface can be easily modified[27] to introduce permselectivity.[28,29] Importantly, the molecular flux normal to the (111) plane of an opal layer remains significant even when the pore size is sufficiently small to impart chemical selectivity.[30]

Recently, we reported[31] on the chiral permselectivity of opal films surface-modified with a chiral selector moiety **1** (Chart 1).[32] We studied the transport of chiral molecules through the chiral opal films using cyclic voltammetry of

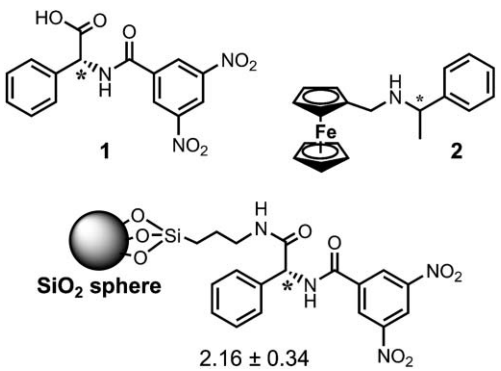

Chart 1 The structure of the chiral selector **1**, the chiral probe molecule **2** and the chiral permselectivity obtained for the chiral selector **1** attached to the silica surface as shown.

Department of Chemistry, University of Utah, Salt Lake City, UT, USA. E-mail: i.zharov@utah.edu; Fax: +1 801 581 84333; Tel: +1 801 587 9335

† This paper is part of a *Journal of Materials Chemistry* issue highlighting the work of emerging investigators in materials chemistry.

redox-active chiral probe molecules such as **2** (Chart 1) and its analogues[33] and found a selectivity (molecular flux ratio for *S* and *R* enantiomer, calculated as the ratio of the limiting currents for *S* and *R* enantiomer) of *ca.* 2.2 (Chart 1) that was reversed when the configuration of the selector moiety was changed from *R* to *S*. In addition, we studied the dependence of the flux and selectivity on the concentration of the permeants and found that at low concentrations the molecular flux increases linearly with the concentration and becomes saturated at higher concentrations. Thus, we concluded that permselectivity in the chiral opal films is governed by surface transport in a way similar to that demonstrated in polymer membranes[23,34] and surface-modified nanotubes.[24]

In order to gain further insight into the molecular transport mechanism in chiral nanoporous opal films, and to improve their selectivity, we carried out a systematic study of the permselectivity as a function of film geometry, solvent, supporting electrolyte concentration, the structure of the linker and of the chiral selector moiety using the chiral probe molecule **2**. The results of this study are described below.

Experimental

Materials

The following reagents were obtained from Sigma-Aldrich, Inc. and used without further purification: tetraethoxysilane (TEOS), 3-aminopropyltriethoxysilane, phenylglycine, 3,5-dinitrobenzoyl chloride, *R*-(+)-α-methylbenzylamine hydrochloride, ferrocene aldehyde, *R*-phenylglycine and benzoylchloride. *N*-α-Methyl-D-valine hydrochloride was received from EMD Biosciences, Inc., and 4-aminobutyl-triethoxysilane, *N*-(2-aminoethyl)-3-aminopropyl-triethoxysilane and aminoethyl-(aminomethyl)-phenyl-trimethoxysilane were obtained from Gelest, Inc. Reagent grade solvents were used except for absolute ethanol, anhydrous MeOH, acetonitrile, dichloromethane and dimethylsulfoxide (DMSO) distilled from CaH_2, and THF distilled from Na/benzophenone.

Characterization

NMR spectra were recorded using a Varian VXL-300 or a Varian Unity-300 at 300 MHz for ^1H and 75 MHz for ^{13}C. Mass spectra were obtained using a Finnigan MAT95. Dynamic light scattering (Brookhaven ZetaPALS) and scanning electron microscopy (Hitachi S3000-N) were used to perform size characterization of the silica spheres. UV spectra were recorded using an Ocean Optics USB2000 instrument.

Pt microdisk electrodes

Pt microdisk electrodes (25 μm in diameter) shrouded in glass were prepared by first attaching a 1.0 mm diameter Cu wire (Alfa Aesar) to a 25 μm diameter Pt wire using Ag paint (DuPont). The Pt wire was then flame-sealed in a glass capillary; the capillary was bent to a U-shape and the end cut orthogonal to the length of the capillary with a diamond saw to expose the Pt disk. The resulting electrodes were then polished with microcut paper disks (Buehler), from 240 to 1200 grit in succession, until the surface was free from visible defects.

Preparation of the opal films

Silica spheres of 200 ± 5 and 440 ± 11 nm in diameter were prepared by rapidly adding a solution of tetraethoxysilane (TEOS) in absolute ethanol to a stirred solution of ammonia and water in absolute ethanol at room temperature. The sphere size is determined by the final concentration of the components, for 200 nm spheres it was 0.2 M TEOS, 0.4 M ammonia and 17 M water, and for 440 nm spheres it was 0.2 M TEOS, 1.1 M ammonia and 17 M water. The size and size uniformity of the spheres were verified by SEM.

The opal films were deposited onto the glass-shrouded Pt electrodes by placing them into 3 DR Fisher vials filled with 1.5 or 3.0 wt% colloidal solutions of the spheres in EtOH. The vials were placed under a crystallization dish and the solutions were allowed to evaporate at room temperature for 2–3 days in a vibration-free environment.

Amine modification of the opal membranes was achieved by immersing the electrodes with pre-assembled opals in an unstirred 0.056 M solution of 3-aminopropyltriethoxysilane, 4-aminobutyltriethoxysilane (**3**), 2-(2-amino-ethylamino)-ethyl-triethoxysilane (**4**) or 2-{3-[(2-amino-ethylamino)-methyl]-phenyl}-ethyltrimethoxysilane (**5**) in dry acetonitrile at room temperature for 17 hours (stirring the solution led to damaging the membranes) followed by soaking the electrodes in dry acetonitrile for 1 hour. The presence of the surface amino groups was confirmed by treating the silica spheres with dansyl chloride, followed by fluorescence measurements.

(3,5-Dinitro-benzoylamino)-phenylacetic acid (1)

Both *R* and *S* enantiomers of compound **1** were prepared following the literature procedure.[32] A mixture of phenylglycine (23 mmol, 1.1 equivalents) and 3,5-dinitrobenzoyl chloride (22 mmol, 1.0 equivalent) in 50 mL of dry tetrahydrofuran (THF) was stirred for 1 week at room temperature. The *R* and *S* enantiomers of phenylglycine were utilized individually to prepare the respective enantiomerically pure compounds. Following 1 week of stirring, the solvent was evaporated from the creamish cloudy mixture, and the residue was dissolved in 50 mL of 5% aqueous $NaHCO_3$. The aqueous solution was extracted with diethyl ether (2 × 100 mL), acidified to pH = 5.0, and washed with ether until no more material could be extracted into ether. The organic extracts were combined and concentrated on the rotary evaporator to yield a cream-colored solid. Crystallization in a minimal amount of MeOH afforded the enantiomerically pure compound **1** in 92% yield as a cream-colored solid. NMR and IR spectra of **1** were identical to those reported in the literature.

Ferrocen-2-ylmethyl-(1-phenyl-ethyl)-amine (2)

A published procedure was used for the preparation of compound **2**.[33] Methylbenzylamine hydrochloride (*R* and *S* enantiomers of the amino acid hydrochloride were utilized individually to prepare the respective enantiomerically pure compounds), triethylamine, and ferrocene aldehyde (1 equivalent each, 2 mmol) were dissolved in dry $CHCl_3$. Following 3 h of reflux the reaction mixture was allowed to cool to room temperature and the solvent was evaporated *in vacuo* to

quantitatively yield the imine as a yellow solid. Without further purification, the imine was dissolved in 20 mL dry of CH_3OH and this solution was cooled to 0 °C with stirring. $NaBH_4$ (4 equivalents, 8 mmol) was carefully added to the reaction mixture in small portions with stirring at 0 °C. Following the addition of $NaBH_4$, the reaction mixture was allowed to stir at 0 °C. After 30 min, 20 mL of 1 M aqueous NaOH was added to the reaction mixture and the organic phase was extracted with $CHCl_3$ (3 × 100 mL). The combined organic phases were evaporated to dryness to provide the pure ferrocene methyl amino acid **2** as a yellowish-brown oil in 90% yield. The synthesized compounds required no further purification. NMR and IR spectra of **2** were identical to those reported in the literature.

Benzoylamino-phenylacetic acid (7)

A mixture of *R*-phenylglycine (5.3 mmol, 1.1 equivalents) and benzoylchloride (5.0 mmol, 1.0 equivalent) in 25 mL of dry THF was stirred for 1 week at room temperature. The solvent was then evaporated from the creamish cloudy mixture, and the residue was dissolved in 20 mL of 1 M aqueous NaOH. The aqueous solution was extracted with ether (2 × 100 mL) and ethyl acetate (2 × 100 mL). The organic extracts were combined and concentrated in vacuo to yield a cream-colored solid. Crystallization in a minimal amount of methanol afforded the enantiomerically pure compound **7** in a 83% yield as a cream-colored solid. ^{1}H NMR (300 MHz, $CDCl_3$): δ 8.06 (d, 2H), 7.96 (d, 2H), 7.64–7.35 (m, 8H), 5.77 (s, 1H). ^{13}C NMR (75 MHz, $CDCl_3$): δ 176.9, 172.6, 134.1, 132.2, 130.4, 129.5, 129.3, 129.1, 128.9, 128.7, 127.6, 127.4, 57.2.

2-Benzoylamino-3-methylbutyric acid (8)

A mixture of *N*-α-methyl-D-valine hydrochloride (3.7 mmol, 1.1 equivalents) and benzoylchloride (3.5 mmol, 1.0 equivalents) in 25 mL of dry methylene chloride was stirred for 5 min, followed by the addition of *N,N*-diisopropylethylamine (3.5 mmol, 1.0 equivalent). The reaction mixture was stirred at room temperature for 24 h after which a pink solution was recovered and the methylene chloride was evaporated. The residue was dissolved in 15 mL of 1 M aqueous sodium hydroxide and the aqueous solution was extracted with ether (3 × 100 mL). The organic layer was evaporated to afford the crude product as a brown oil. The crude product was purified *via* column chromatography using a 50:50 mixture of ethyl acetate:hexane as the elutent. Chromatography afforded the enantiomerically pure compound **8** as yellow crystals in a 87% yield. ^{1}H NMR (300 MHz, $CDCl_3$): δ 8.15 (dd, H), 7.96 (d, 2H), 7.70–7.53 (m, 3 H), 4.98 (s, H), 3.66 (m, H), 3.10 (m, H), 1.45 (d, 6H). ^{13}C NMR (75 MHz, $CDCl_3$): δ 172.5, 162.6, 134.8, 130.8, 130.6, 162.6, 129.5, 129.1, 128.7, 61.7, 30.5, 29.9, 29.6. MS (CI): *m*/*z* 236 ($[M + H]^+$).

Preparation of chiral opal films

Chiral modification of the amine modified opal membranes was achieved by immersing the electrodes with pre-assembled amine modified opals in an unstirred, equimolar solution (0.065 M), of compound **1**, **6**, **7** or **8** and *N*-ethoxycarbonyl-2-ethoxy-1,2-dihydroquinoline (EEDQ) in dry THF at room temperature for 24 h. The resulting chiral opal electrodes were then soaked in CH_2Cl_2 for 1 h.

Surface coverage of chiral selector

To determine the surface coverage of the amine modified opal film with compounds **1**, **6**, **7** and **8** they were dissolved in 9.9 mL $CHCl_3$ and 0.1 mL DMSO to afford a stock 1 mM solution. Their extinction coefficients at 300 nm were determined by UV measurements at concentrations ranging from 0.1 to 0.5 mM. Next, UV spectra were obtained for colloidal solution of silica spheres modified with these compounds. Based on the absorbance at 300 nm, the surface coverage was estimated using 2.2 g cm^{-3} density for silica spheres. Surface coverage was calculated to be 6–8 molecules nm^{-2}.

CV measurements

The flux of permeants across the opal film was measured voltammetrically using a 2-electrode cell and an Ag/AgCl reference/counter electrode. A Par Model 175 Universal Programmer and Dagan Cornerstone Chem-Clamp potentiostat were used to conduct the measurements. Data were recorded with a PC using programs written in LabView 7.0. All solutions were purged with N_2 to remove dissolved O_2. The voltammetric response of the bare, opal-modified, and chiral-modified Pt electrodes was measured in 1×10^{-3} M solutions for *R* and *S* enantiomers of compound **2** and ferrocene, utilizing 0.1 M tetrabutylammonium phosphohexafluoride (TBAPF) as supporting electrolyte. We found this supporting electrolyte concentration to be the most suitable for the measurements since at concentrations below 0.1 M cyclic voltammograms became extremely noisy. The limiting current ratio for the enantiomers did not seem to be affected by the supporting electrolyte concentration. We repeated these experiments with six different electrodes, obtaining semi-quantitative reproducibility in the absolute and relative changes in i_{lim} following deposition of the opal and chemical modification of the silica surface.

Results and discussion

Opal film geometry

In order to determine if the film thickness and nanopore size of the opal films affect the chiral permselectivity, we assembled opal films using 440 nm diameter silica spheres to roughly double the pore size compared to those in the opal formed from 200 nm spheres, and utilized a 3.0 wt% colloidal solution of 200 nm and 440 nm silica spheres respectively (as opposed to the 1.5 wt% solution that has been originally used) to double the thickness of the opal film. Both types of films were modified with **1*R***. We obtained a selectivity of *ca.* 2.1–2.3 for enantiomers of **2** using the thicker opal films, and a selectivity of *ca.* 1.6 for enantiomers of **2** using the opal film with larger nanopores. Based on these results, we conclude that the film thickness does not significantly affect the permselectivity of the chiral opals, while increasing the nanopore size decreases the selectivity to a measurable extent, suggesting that a through-solution diffusion of permeants starts

playing a part in the overall transport through the opal films containing larger nanopores.

Solvent polarity

According to the three-point theory of chiral separations,[5] the selectivity results from non-covalent interactions, such as hydrogen bonding and π–π stacking, between the permeating enantiomers and the surface-bound chiral selector moieties. Thus, solvents capable of disrupting these interactions might affect the chiral selectivity in opal films. In order to explore the solvent effect on the chiral permselectivity we studied the transport of enantiomers of **2** through opal films modified with **1R** in four different solvents: dichloromethane, acetonitrile (MeCN), THF and DMSO. The selectivities obtained in these solvents were 2.16 ± 0.34, 2.23 ± 0.01, 1.47 ± 0.01 and 1.31 ± 0.02 respectively. No correlation can be seen between the chiral permselectivity and such common solvent polarity parameters as dielectric constant or E_T.[35] However, it is clear that the selectivities in dichloromethane and MeCN are quite similar, while they are significantly reduced in THF and DMSO to very similar values. It appears that the hydrogen donor ability of the solvent plays the most important role, as the donor numbers for THF and DMSO,[35] both oxygen-containing solvents, are significantly higher than those of dichloromethane and MeCN. Thus, it is expected that the highest enantiomeric permselectivity in chiral opal films would be achieved in non-polar, non-donor solvents.

Linker structure

Next, we varied the length and structure of the linker[36] attaching the chiral selector moiety **1** to the silica surface with the expectation that placing the chiral selector moiety away from the surface might improve its ability to interact with permeating molecules, and thus improve the selectivity. The structures of the linkers are shown in Chart 2 together with the corresponding selectivities obtained using the chiral probe **2**. In order to verify that only the primary amine of the linker was coupled to the chiral selector moiety in the case of compounds **4** and **5**, we treated them in solution with the chiral selector **1** under the conditions used for the surface modification, and determined by NMR that only one chiral selector moiety was attached. Thus, the linker/selector assemblies **1**, **3–5** differ in the overall length of the chain in all cases, in one additional secondary amino group in the case of **4**, and in the case of **5** in both an additional secondary amino group and a phenyl group.

Introducing a slightly longer linker, *i.e.*, **3**, does not lead to a significant increase in chiral selectivity compared to **1**. Furthermore, introducing much longer linkers carrying additional functional groups capable of hydrogen bond formation and π–π stacking interactions either does not increase the chiral selectivity to a large extent (as in the case of **5**), or leads to a significant decrease in the selectivity (*i.e.*, in the case of **4**). The origins of the different selectivities for the seemingly similar linkers **4** and **5** are not presently clear.

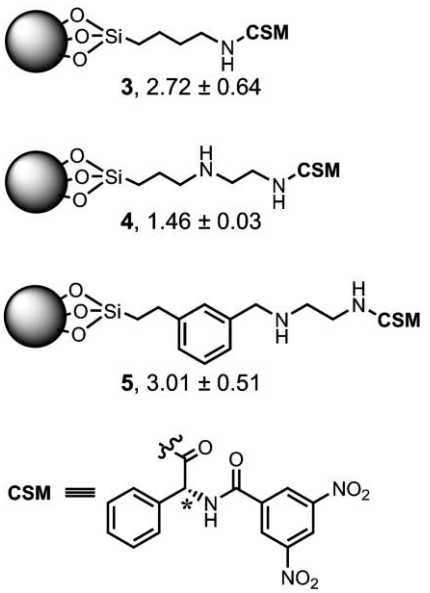

Chart 2 Structures of the linker moieties used to attach the chiral selector moiety **1** to the opal nanopore surfaces, and the corresponding chiral permselectivities obtained for the chiral probe **2**.

Chiral selector structure

Finally, we explored the influence of the chiral selector structure on the permselectivity while maintaining the length of the linker constant at three carbon atoms. The structures of the chiral selectors are shown in Chart 3 together with the corresponding selectivities obtained using the chiral probe **2**, and the corresponding voltammograms are shown in Fig. 1.

The surface coverage of the silica spheres modified with the chiral selector moieties **6–8** in a colloidal solution under the conditions identical to those used for the opal film modification was determined by UV spectroscopy to be *ca.* 6–8 chiral moieties per nm^2. This value is *ca.* two times higher than the typical number of hydroxyl groups on a silica surface,[37] and likely reflects the formation of a homo-condensed or an anarchically grafted hybrid phase during the amine modification of the silica spheres.[28,29] As we reported earlier,[31] upon opal film modification the limiting current of ferrocene decreases by *ca.* 75%. We attributed this drop in i_{lim} to the nanopore size reduction as a result of the surface modification with multiple layers of grafted aminosilane and the chiral selector moieties. Using the relationship between the limiting current and opal void fraction,[38,39] and straightforward geometrical considerations,[40] we estimated the nanopore size inside the chiral opal film as 6.4 nm, compared to 16 nm for the unmodified opal film. The extent to which the surface

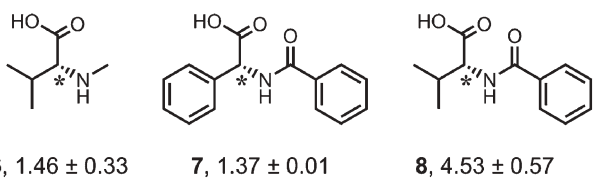

Chart 3 Structures of the chiral selectors and the corresponding chiral permselectivities obtained for the chiral probe **2**.

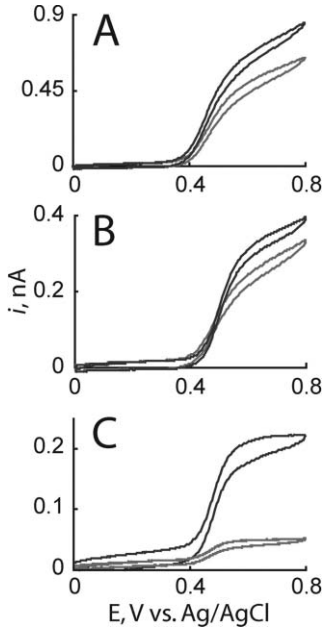

Fig. 1 Overlay of voltammetric responses of a Pt electrode for **2*S*** (black) and **2*R*** (grey) after the opal film surface modification with **6*R*** (A), **7*R*** (B) and **8*R*** (C).

amino groups are modified with the chiral selector moieties is presently unknown. This parameter will be further investigated as increasing, if possible, the surface coverage might provide additional improvements to the chiral selectivity of the opal films.

When commercially available chiral molecule **6** is used to modify the aminated opal film surface, the chiral selectivity significantly decreases, likely as a result of losing the functionality responsible for π–π stacking ability of the chiral selector, in accord with the chiral separations theory.[5] Removing the nitro groups from the amide portion of the chiral selector (compound **7**), which should lead to a decrease in its π-acceptor ability, results in a similar decrease in chiral selectivity. This observation is in line with the chiral separations theory[5] and it also suggests that the amide phenyl ring plays an important role in the chiral recognition. Surprisingly, replacing the amino acid phenyl ring by an isopropyl group (compound **8**) does not result in further decrease in the chiral selectivity, but leads to the opposite effect, *increasing* the chiral selectivity more than two-fold compared to that of **1**. This observation suggests that the amino acid phenyl ring plays a minor role in the chiral recognition mechanism, but its steric bulk might interfere with the non-covalent interactions of the chiral selector moiety with the permeants. Thus, future designs of the chiral selectors for opal membranes will focus on altering the amide aromatic ring of the chiral selector moieties by changing its steric and electronic properties. The chiral selectivity of 4.5 found for the chiral selector **8** is one the highest reported for chiral membranes.[6]

Conclusions

The chiral permselectivity in thin opal films modified with chiral selector moieties on the silica surface was studied as a function of opal film geometry, supporting electrolyte concentration, solvent polarity, and chiral selector and linker structure. While the opal film thickness, supporting electrolyte concentration and linker length and structure (with one exception) did not have a significant influence on the chiral permselectivity, the nanopore size, solvent polarity and selector structure had a pronounced effect. These observations are in agreement with the chiral selectivity mechanism in the opal films in which the permeating enantiomers are transported with different rates through the surface utilizing non-covalent interactions between the chiral permeant molecules and surface-bound chiral selectors. The chiral selectivity (transport rate ratio for *S* and *R* enantiomers) achieved in the present study was 4.5, which is one of the highest reported for chiral membranes.

Acknowledgements

This work was supported by the ACS Petroleum Research Fund. I. Z. is grateful to the Camille and Henry Dreyfus Foundation for a New Faculty Award.

References

1 http://www.fda.gov/cder/guidance/stereo.htm (accessed 29th November 2006).
2 C. A. M. Afonso and J. G. Crespo, *Angew. Chem., Int. Ed.*, 2004, **43**, 5293–5295.
3 J. E. Rekoske, *AIChE J.*, 2001, **47**, 2–5.
4 K. B. Jirage and C. R. Martin, *Trends Biotechnol.*, 1999, **17**, 197–200.
5 W. H. Pirkle and T. C. Pochapsky, *Chem. Rev.*, 1989, **89**, 347–362.
6 B. Chankvetadze, *Chiral Separations*, Elsevier, Amsterdam, 2001.
7 H. Y. Aboul-Enein and I. Ali, *Chiral Separations by Liquid Chromatography and Related Techniques*, Marcel Dekker, New York, NY, 2003.
8 *Chiral Separation Techniques. A Practical Approach*, ed. G. Subramanian, Wiley-VCH, New York, 2001.
9 O. A. Hazzazi, G. A. Attard and P. B. Wells, *J. Mol. Catal. A: Chem.*, 2004, **216**, 247–255.
10 M. Yoshikawa and K. Yonetani, *Desalination*, 2002, **149**, 287–292.
11 P. Hadik, L.-P. Szabo and Z. Farkas, *J. Membr. Sci.*, 2005, **251**, 223–232.
12 N. H. Lee and C. W. Frank, *Polymer*, 2002, **43**, 6255–6262.
13 T. Aoki, M. Teraguchi, S. Kim, T. Kaneko and S. Hadano, *Macromolecules*, 2005, **38**, 6367–6373.
14 J. Randon, F. Garnier, J. L. Rocca and B. Maisterrena, *J. Membr. Sci.*, 2000, **175**, 111–117.
15 S. Kiyohara, M. Nakamura, K. Saito, K. Sugita and T. Sugo, *J. Membr. Sci.*, 1999, **152**, 143–149.
16 T. Aoki, S. Tomizawa and E. Oikawa, *J. Membr. Sci.*, 1995, **99**, 117–125.
17 C. Minguillon, T. Gumi and C. Palet, *Polymer*, 2005, **46**, 12306–12312.
18 M. Yoshikawa, T. Ooi and J. Izumi, *Eur. Polym. J.*, 2001, **37**, 335–342.
19 T. Aoki, M. Ohshima, K. I. Shinohara, T. Kaneko and E. Oikawa, *Polymer*, 1997, **38**, 235–238.
20 A. Maruyama, N. Adachi, T. Takatsuki, M. Torii, K. Sanui and N. Ogata, *Macromolecules*, 1990, **23**, 2748–2752.
21 E. Yashima, J. Noguchi and Y. Okamoto, *J. Appl. Polym. Sci.*, 1994, **54**, 1087–1091.
22 M. Yoshikawa, J. Izumi, T. Kitao, S. Koya and S. Sakamoto, *J. Membr. Sci.*, 1995, **108**, 171–175.
23 H. H. Rmaile and J. B. Schlenoff, *J. Am. Chem. Soc.*, 2003, **125**, 6602–6603.
24 S. B. Lee, D. T. Mitchell, L. Trofin, T. K. Nevanen, H. Söderlund and C. R. Martin, *Science*, 2002, **296**, 2198–2201.
25 B. B. Lakshmi and C. R. Martin, *Nature*, 1997, **388**, 758–760.

26 S. Wong, V. Kitaev and G. A. Ozin, *J. Am. Chem. Soc.*, 2003, **125**, 15589–15598.
27 B. J. Ravoo, D. N. Reinhoudt and S. Onclin, *Angew. Chem., Int. Ed.*, 2005, **44**, 6282–6304.
28 M. R. Newton, A. K. Bohaty, H. S. White and I. Zharov, *J. Am. Chem. Soc.*, 2005, **127**, 7268–7269.
29 M. R. Newton, A. K. Bohaty, H. S. White and I. Zharov, *Langmuir*, 2006, **22**, 4429–4432.
30 M. R. Newton, K. A. Morey, Y. Zhang, R. J. Snow, M. Diwekar, J. Shi and H. S. White, *Nano Lett.*, 2004, **4**, 875–880.
31 J. Cichelli and I. Zharov, *J. Am. Chem. Soc.*, 2006, **128**, 8130–8131.
32 W. H. Pirkle, D. W. House and J. M. Finn, *J. Chromatogr.*, 1980, **192**, 143–158.
33 A. Hess, J. Sehnert, T. Weyhermueller and N. Metzler-Nolte, *Inorg. Chem.*, 2000, **39**, 5437–5443.
34 T. R. Farhat and J. B. Schlenoff, *J. Am. Chem. Soc.*, 2003, **125**, 4627–4636.
35 T. H. Lowry and K. S. Richardson, *Mechanism and Theory on Organic Chemistry*, 3rd edn, Harper Collins, New York, 1987.
36 S. Fiorilli, B. Onida, C. Barolo, G. Viscardi, D. Brunel and E. Garrone, *Langmuir*, 2007, **23**, 2261–2268.
37 P. K. Jal, S. Patel and B. K. Mishra, *Talanta*, 2004, **62**, 1005–1028 and references therein.
38 A. J. Bard and L. R. Faulkner, *Electrochemical Methods: Fundamentals and Applications*, 2nd edn, Wiley, New York, 2001.
39 E. L. Cussler, *Diffusion. Mass Transfer in Fluid Systems*, 2nd edn, Cambridge University Press, Cambridge, UK, 1997.
40 O. Schepelina and I. Zharov, *Langmuir*, 2006, **22**, 10523–10527.